

Semi-classical treatment of k -essence effect on cosmic temperature

Abhijit Bandyopadhyay¹, Debashis Gangopadhyay² and Arka Moulik³

Department of Physics
Ramakrishna Mission Vivekananda University
Belur Math, Howrah 711202, India

Abstract

A phenomenological model is described for Cosmic Microwave Background Radiation (CMBR) evolution with dark energy an essential ingredient in the form of a k -essence scalar field. The following features of this evolution can be successfully obtained from this model: (a) the *observed* variation of the rate of change of scale factor $a(t)$, i.e. \dot{a} , with time and (b) the *observed* value of the epoch when the universe went from a decelerating phase to an accelerated phase. These two features have been matched with graphical transcriptions of SNe Ia data. The model also indicates that the evolution is sensitive to the presence of inhomogeneity and this sensitivity increases as one goes further into the past. Further, the value of the inhomogeneity parameter determines the epoch of switch over to an accelerated phase. A positive value of inhomogeneity parameter leads to switch over at earlier epochs, while a negative value leads to switch over at later epochs. If the value of the inhomogeneity parameter is a bit negative then the crossover point from deceleration to acceleration gives better agreement with the observed value.

1 Introduction

Observations of luminosity distances of the type Ia Supernovae (SNe Ia) [1, 2, 3, 4, 5, 6, 7, 8, 9, 10, 11, 12, 13] indicate that the universe is presently undergoing a phase of accelerated expansion. Overwhelming support exists from other independent observations like Cosmic Microwave Background anisotropies measured with WMAP satellite [14] and Planck satellite [15], Baryon Acoustic Oscillations (BAO) [16, 17, 18] and measurement of oscillations present in the matter power spectrum through large scale surveys [19].

One of the theoretical approaches in explaining the observed late time acceleration of the universe is the presence of dark energy which correspond to a negative pressure in the ideal perfect fluid model of a Friedmann-Lemaître-Robertson-Walker (FLRW) universe. Recent measurements in Planck Satellite experiment [15] suggest dark energy contributes 68.3% of the total content of present universe. The issue of origin of dark energy can be addressed in the framework of k -essence scalar field model of dark energy which involve actions with non-canonical kinetic terms. In a k -essence scalar field model, the kinetic energy dominates over the potential energy associated with the scalar field. Literature on dark energy and k -essence models can be found in [20, 21, 22, 23, 24].

To begin with (Sec. 2), we shall consider a model [25] where the scalar field is homogeneous, i.e. $\phi(t, \mathbf{x}) \equiv \phi(t)$ and the FLRW metric has zero curvature constant, i.e. the universe is flat. A Lagrangian

¹Email: abhijit@rkmu.ac.in

²Email: debashis@rkmu.ac.in

³Email: arkamoulik@rkmu.ac.in

for the k -essence field that we shall use has [25] two generalised coordinates $q(t) = \ln a(t)$ ($a(t)$ is the scale factor) and a scalar field $\phi(t)$ with a complicated polynomial interaction between them. In this Lagrangian, q has a standard kinetic term while ϕ does not have a kinetic part and occurs purely through the interaction term. The general form of k -essence Lagrangian is assumed to be a function $L = -V(\phi)F(X)$ with $X = \frac{1}{2}g_{\mu\nu}\nabla^\mu\phi\nabla^\nu\phi$ where ∇^μ is the covariant derivative, X does not depend explicitly on ϕ to start with and $V(\phi)$ is taken to be a constant. In [26], X was shown to satisfy a general scaling relation, *viz.* $X(\frac{dF}{dX})^2 = Ca(t)^{-6}$ with C a constant. [25] incorporates the scaling relation of [26].

In [27] it was shown that the Lagrangian in the above model, under certain assumptions reduces to that of a harmonic oscillator on the half-plane with time dependent frequency. The quantum mechanical amplitude for q to evolve from a value $q_a(t_a)$ to $q_b(t_b)$ was computed and using the fact that the scale factor $a(t)$ is inversely proportional to the cosmic temperature T_a at a given epoch t_a , the quantum amplitude is transformed into an amplitude for evolving from $\ln T_a$ to $\ln T_b$ (Sec. 2).

In this work we shall show that the above quantum mechanical amplitude is a plausible phenomenological model of CMBR evolution.

Again, the latest results obtained from the Planck probe [15] have firmly established that inhomogeneity effects in CMBR do not have their origins in non-gaussianities. Hence alternative theoretical approaches to inhomogeneities are desirable. In this context we shall show that a phenomenological input can be introduced in the above model to take into account inhomogeneities. This is done by making the scalar field inhomogeneous (Sec. 2).

This phenomenological model has been developed along the following lines keeping the observational scenario in mind. First a combined analysis of SNe Ia data and Observational Hubble data is done to obtain graphical transcriptions of (a) the behaviour of the scale factor $a(t)$ with time (b) the behaviour of the rate of change of scale factor $\dot{a}(t)$ with time and (c) the second derivative of $a(t)$ with respect to time *viz.* $\ddot{a}(t)$.

The observational values thus obtained are then used as inputs in the model described as follows. Values of $a(t)$ obtained at specific epochs are plugged into the expression for the quantum amplitude to obtain the probability profile of the evolution with time. The obtained profile is then like the profile of the expectation value of microscopic quantum fluctuations, remembering that the expectation value is proportional to the transition probability.

The following features of this evolution can be successfully obtained from this model:

- (a) The *observed* variation of the rate of change of scale factor $a(t)$, i.e. \dot{a} , depicted in middle panel of Fig. 2, *matches with the probability profile obtained theoretically from the model* after plugging in observed values of \dot{a} at corresponding epochs, Fig. 4.
- (b) The *observed* value of the epoch when the universe went from a decelerating phase to an accelerated phase, Fig. 2, *is nearly the same as obtained from the theoretically obtained profile*, Fig. 4.
- (c) There is a qualitative indication that the probability is sensitive to the presence of inhomogeneity. This sensitivity increases as one goes further into the past. This is seen in Fig. 4 and 6 where the solid line represents homogeneity while the dotted lines denote the presence of inhomogeneity.
- (d) The value of the inhomogeneity parameter determines the epoch of switch over to an accelerated phase. A positive value leads to switch over at earlier epochs, while a negative value leads to switch over at later epochs.

- (e) If the value of the inhomogeneity parameter is a bit negative then the crossover point from deceleration to acceleration gives better agreement with the observed value. The homogeneous case (solid line in the figure) seems to be roughly the mean curve with respect to positive and negative values for the inhomogeneity parameter. This is seen in Fig. 6.

2 Formalism : k -essence Lagrangian for scalar field

We recall briefly the content of references [25, 27]. The Lagrangian L (or the pressure p) is taken as

$$L = -V(\phi)F(X) \quad (1)$$

The energy density is

$$\rho = V(\phi)[F(X) - 2XF_X] \quad (2)$$

with $F_X \equiv \frac{dF}{dX}$ and in the present work $V(\phi) = V$ is a constant (> 0).

For a flat FLRW metric the equation for the k -essence field is

$$(F_X + 2XF_{XX})\ddot{\phi} + 3HF_X\dot{\phi} + (2XF_X - F)\frac{V_{\phi}}{V} = 0 \quad (3)$$

$H = \dot{a}(t)/a(t)$ is the Hubble parameter. Isotropy and homogeneity imply $\phi(x, t) \equiv \phi(t)$, and so $X = \frac{1}{2}\dot{\phi}^2$. For $V(\phi) = \text{constant}$, one has the scaling law solution [26]

$$XF_X^2 = Ca^{-6} \quad (4)$$

Using Eq. (4), the zero-zero component of Einstein's field equations and homogeneity and isotropy an expression for the Lagrangian is obtained as [25]

$$L = -c_1\dot{q}^2 - c_2V\dot{\phi}e^{-3q} \quad (5)$$

where $a(t) = e^{q(t)}$, $c_1 = 3(8\pi G)^{-1}$, $c_2 = 2\sqrt{C}$, (we shall always take the positive square root of C) and the scalar potential V is a constant.

Smaller values of q mean that we are going back to smaller values of a i.e. to earlier epochs. Expanding the exponential and keeping terms up to $\mathcal{O}(q^2)$ one has [27]

$$L = -\frac{M}{2}\left[\dot{q}^2 + 12\pi Gg(t)q^2\right] - \frac{1}{2}g(t) \quad (6)$$

where $M = \frac{3}{4\pi G} = \frac{3m_{\text{Pl}}^2}{4\pi}$, $g(t) = 2\sqrt{C}V\dot{\phi}$, m_{Pl} is the Planck energy and we use $\hbar = c = 1$ (c is speed of light, \hbar is Planck's constant). The last term, $\frac{1}{2}g(t)$, is a total derivative. Dropping this term and the minus sign in front we finally write the Lagrangian as

$$L = \left(\frac{3}{8\pi G}\right)\left[\dot{q}^2 + \left\{24\pi G\sqrt{C}V\dot{\phi}\right\}q^2\right] \quad (7)$$

A possible solution for q is obtained when $-24\pi G\sqrt{C}V\dot{\phi}$ is a positive number. Writing $\frac{3}{4\pi G} = \frac{3m_{\text{Pl}}^2}{4\pi} \equiv M$ and $-24\pi G\sqrt{C}V\dot{\phi} \equiv \Omega^2(t)$ (Ω is real), we rewrite the Lagrangian as

$$L = \frac{M}{2}\left[\dot{q}^2 - \Omega^2(t)q^2\right] \quad (8)$$

The harmonic oscillator with time-dependent frequency (Eq. 8) can now be used as our cosmological model for estimating quantum fluctuations of the temperature using path integral technique. Write the dynamical variable as $q(t) = q_{cl}(t) + y(t)$ where $y(t)$ ($0 < y(t) < \infty$) is the fluctuation over the classical value $q_{cl}(t)$. This corresponds to a time dependent oscillator in the half plane [28, 29, 30, 31]. Then the quantum mechanical amplitude for q to evolve from a value $q_a(t_a)$ to $q_b(t_b)$ is given by [32]

$$\langle q_a, t_a | q_b, t_b \rangle = F(t_b, t_a) \exp \left(\frac{i}{\hbar} S_{cl} \right) \quad (9)$$

where $S_{cl} = \int_{t_a}^{t_b} L_{cl} dt = \int_{t_a}^{t_b} dt \frac{M}{2} [\dot{q}_{cl}^2 - \frac{1}{2} \Omega^2(t) q_{cl}^2]$ and $F(t_a, t_b)$ is calculated following [28]. The fluctuations $y(t)$ satisfy the differential equation

$$\ddot{y} + \Omega^2(t)y = 0, \quad (10)$$

which will have quasi-periodic solutions for real Ω . Consider two independent quasi-periodic solutions of Eq. (10)

$$y_1(t) = \psi(t) \sin \xi(t, t_a) \quad ; \quad y_2(t) = \psi(t) \sin \xi(t_b, t) \quad (11)$$

with the boundary conditions

$$y_1(t_a) = 0 \quad ; \quad y_2(t_b) = 0 \quad (12)$$

and where $\psi(t)$ satisfies the Ermakov-Pinney equation [33]

$$\ddot{\psi} + \Omega^2(t)\psi - \psi^{-3} = 0 \quad (13)$$

with $\xi(t, s)$ defined as

$$\xi(t, s) \equiv \nu(t) - \nu(s) = \int_s^t \psi^{-2}(t') dt' \quad (14)$$

$\psi(t)$ and $\nu(t)$ respectively represent the amplitude and phase of the time dependent oscillator. The fluctuation factor $F(t_b, t_a)$ is then given by

$$F(t_b, t_a) = \left[\frac{M \sqrt{(\dot{\nu}_a \dot{\nu}_b)}}{2\pi i \hbar \sin \xi(t_b, t_a)} \right]^{1/2} \quad (15)$$

So the amplitude is (for relevant boundary conditions $q(t_a) = q_a, q(t_b) = q_b$),

$$\langle q_b, t_b | q_a, t_a \rangle = \left[\frac{M \sqrt{(\dot{\nu}_a \dot{\nu}_b)}}{2\pi i \hbar \sin \xi(t_b, t_a)} \right]^{1/2} \left[\exp \left(\frac{i S_{cl}^+}{\hbar} \right) - \exp \left(\frac{i S_{cl}^-}{\hbar} \right) \right] \quad (16)$$

where

$$S_{cl}^\pm = \left(\frac{\dot{\psi}_b q_b^2}{\psi_b} - \frac{\dot{\psi}_a q_a^2}{\psi_a} \right) + \frac{1}{\sin \xi(t_b, t_a)} \left[(\dot{\nu}_b q_b^2 + \dot{\nu}_a q_a^2) \cos \xi(t_b, t_a) \mp 2 \sqrt{\dot{\nu}_b \dot{\nu}_a} q_b q_a \right] \quad (17)$$

We assume $\dot{\nu} \ll 1$, i.e. time rate of change of phase is small. Also, in a homogeneous universe, the temperature of the background radiation is inversely proportional to the scale factor i.e. $T(t) \sim \frac{1}{a(t)}$.

Then to lowest order in $\dot{\nu}$, one has the probability for the logarithm of scale factor or logarithm of inverse temperature evolution as

$$\begin{aligned}
P(t_b, t_a) \equiv P(b, a) &= |\langle q_a, t_a | q_b, t_b \rangle|^2 \\
&\equiv \left| \left\langle \ln \frac{1}{T_b}, t_b \middle| \ln \frac{1}{T_a}, t_a \right\rangle \right|^2 \\
&= \left(\frac{3m_{\text{pl}}^2}{\pi^2 \hbar^2 c} \right) \left(\frac{q_a^2 q_b^2 (\dot{\nu}_a \dot{\nu}_b)^{3/2}}{\sin^3 \xi(t_b, t_a)} \right) \\
&= \frac{3m_{\text{pl}}^2}{\pi^2} (\ln T_a)^2 (\ln T_b)^2 \frac{(\dot{\nu}_a \dot{\nu}_b)^{3/2}}{\sin^3 \xi(t_b, t_a)}
\end{aligned} \tag{18}$$

where \hbar and c have been put equal to unity. Expanding the function $(\sin \xi)^{-3}$ in a Taylor series about $\xi = 0$ we write

$$\begin{aligned}
P(b, a) &= \frac{3m_{\text{pl}}^2}{\pi^2} (\ln T_a)^2 (\ln T_b)^2 \frac{(\dot{\nu}_a \dot{\nu}_b)^{3/2}}{\xi^3(t_b, t_a)} \left[1 + \frac{1}{2} \xi^2(t_b, t_a) + \frac{17}{120} \xi^4(t_b, t_a) + \dots \right] \\
&= \frac{3m_{\text{pl}}^2}{\pi^2} (\ln T_a)^2 (\ln T_b)^2 \left[p_0(b, a) + p_1(b, a) + p_2(b, a) + \dots \right]
\end{aligned} \tag{19}$$

where

$$p_0(b, a) = \frac{(\dot{\nu}_a \dot{\nu}_b)^{3/2}}{\xi^3(t_b, t_a)}, \quad p_1(b, a) = \frac{1}{2} \frac{(\dot{\nu}_a \dot{\nu}_b)^{3/2}}{\xi(t_b, t_a)}, \quad p_2(b, a) = \frac{17}{120} (\dot{\nu}_a \dot{\nu}_b)^{3/2} \xi(t_b, t_a), \dots \tag{20}$$

Choose

$$\psi(t) = e^{\gamma t} \quad \text{where } \gamma \text{ is a constant and } 0 < \gamma < 1 \tag{21}$$

For this choice of ψ , $\xi(t, s) = \nu(t) - \nu(s) = \int_s^t e^{-2\gamma t} dt = -\frac{1}{2\gamma} [e^{-2\gamma t} - e^{-2\gamma s}]$ and therefore, $\nu(t) = -(1/2\gamma)e^{-2\gamma t}$; $\dot{\nu}(t) = e^{-2\gamma t}$.

Using the above expressions for the choice $\psi(t) = e^{\gamma t}$, and expanding different functions as a polynomial of γ we obtain

$$(\dot{\nu}_a \dot{\nu}_b)^{3/2} = e^{-3\gamma(t_b+t_a)} = \left[1 - 3\gamma(t_b + t_a) + \frac{9}{2}\gamma^2(t_b + t_a)^2 + \dots \right] \tag{22}$$

$$\begin{aligned}
\xi(t_b, t_a) &= \nu(t_b) - \nu(t_a) = \int_{t_a}^{t_b} e^{-2\gamma t} dt \\
&= (t_b - t_a) \left[1 - \gamma(t_b + t_a) + \frac{2}{3}\gamma^2(t_b^2 + t_b t_a + t_a^2) - \dots \right]
\end{aligned} \tag{23}$$

$$\frac{1}{\xi^3} = \frac{1}{(t_b - t_a)^3} \left[1 + 3(t_b + t_a)\gamma + 2[2t_a^2 + 2t_b^2 + 5t_b t_a] \gamma^2 + \dots \right] \tag{24}$$

$$\frac{1}{\xi} = \frac{1}{(t_b - t_a)} \left[1 + (t_b + t_a)\gamma + \frac{1}{3}[t_a^2 + t_b^2 + 4t_a t_b] \gamma^2 + \dots \right] \tag{25}$$

Using Eqs. (22),(23), (24) and (25) we calculate the terms $p_0(b, a)$, $p_1(b, a)$, $p_2(b, a) \dots$ appearing in Eq. (19) as

$$p_0(b, a) = \frac{(\dot{\nu}_a \dot{\nu}_b)^{3/2}}{\xi^3(t_b, t_a)} = \frac{1}{(t_b - t_a)^3} \left[1 - \frac{1}{2}(t_b - t_a)^2 \gamma^2 + \dots \right] \quad (26)$$

$$\begin{aligned} p_1(b, a) &= \frac{1}{2} \frac{(\dot{\nu}_a \dot{\nu}_b)^{3/2}}{\xi(t_b, t_a)} \\ &= \frac{1}{2(t_b - t_a)} \left[1 - 2(t_b + t_a) \gamma + \frac{1}{6} (11t_b^2 + 11t_a^2 + 26t_a t_b) \gamma^2 + \dots \right] \end{aligned} \quad (27)$$

$$\begin{aligned} p_2(b, a) &= \frac{17}{120} (\dot{\nu}_a \dot{\nu}_b)^{3/2} \xi(t_b, t_a) \\ &= \frac{17}{120} (t_b - t_a) \left[1 - 4(t_b + t_a) \gamma + \frac{1}{6} (49t_b^2 + 49t_a^2 + 94t_b t_a) \gamma^2 + \dots \right] \end{aligned} \quad (28)$$

The inhomogeneous situation is obtained when relevant quantities have spatial dependence, i.e. dependence on $\mathbf{x} \equiv (r, \theta, \varphi)$, where (r, θ, φ) being the comoving coordinates appearing in the FLRW metric. Then

$$\begin{aligned} X &= \frac{1}{2} g^{\mu\nu} \partial_\mu \phi \partial_\nu \phi \\ &= \frac{1}{2} \left[(\partial_t \phi)^2 - \frac{1}{a^2} (\partial_r \phi)^2 - \frac{1}{a^2 r^2} (\partial_\theta \phi)^2 - \frac{1}{a^2 r^2 \sin^2 \theta} (\partial_\varphi \phi)^2 \right] \end{aligned} \quad (29)$$

Now, for k -essence fields the kinetic energy term dominates over the potential energy i.e. $|\partial_t \phi|^2$ dominates over the square of the r , θ and φ derivatives of the field ϕ , so that, $X \approx \frac{1}{2} \dot{\phi}^2(t, \mathbf{x})$. We write $\phi(t, \mathbf{x}) = \phi(t) \cdot \phi_1(\mathbf{x}) = \phi(t) \cdot (1 + g(\mathbf{x})) \sim \phi(t)(1 + f)$, where we have assumed an expansion $g(x) = \sum f_n x^n$, $n = 0, \dots, \infty$ with $f_0 \equiv f$. The thing to remember is that f is always nonzero and small i.e. $0 < |f| < 1$ in presence of small inhomogeneity and the situation of f being zero means homogeneous universe. Hence in this work the inhomogeneity is introduced through a phenomenological parameter whose non zero value signifies the presence of inhomogeneity. Here the inhomogeneity is introduced through a function which need not be well behaved *everywhere* so that it need not be constant. However, the first term in the series expansion of this (analytic) function is non-zero, more specifically is small i.e. lies between zero and unity. This particular approach will ensure a phenomenological computation of effects of inhomogeneity. In this work, we are working out the zeroth order (in spatial dependence) correction. But the formalism is sufficiently general to calculate up to higher orders. We then have $X = \frac{1}{2} \dot{\phi}^2 (1 + f)^2$ and for constant $V(\phi)$ the form of the Eq. (3) still remains the same and the validity of the scaling relation $X F_X^2 = C a^{-6}$ is again ensured. Moreover, in the derivation of Eq. (4), nowhere was it assumed that ϕ is homogeneous. The crucial assumption was that $V(\phi)$ is a constant. So, the presence of inhomogeneity does not change the scaling relation.

Imposing these constraints the Lagrangian Eq. (7) reduces to

$$L = -\sqrt{2C} a^{-3} V(\partial_t \phi(t, \mathbf{x})) - \left(\frac{3}{8\pi G} \right) H^2 \quad (30)$$

where we have dropped a total derivative term as before. Writing $\phi(t, \mathbf{x}) \sim \phi(t)(1 + f)$ and proceeding

as in the previous section taking $V(\phi) = \text{constant} = V$ we have

$$\begin{aligned}
L &= \frac{M}{2} \left[\dot{q}^2 + \left\{ 24\pi G \sqrt{C} V \dot{\phi} \right\} (1+f) q^2 \right] \\
&= \frac{M}{2} \left[\dot{q}^2 - \Omega^2(t) (1+f) q^2 \right] \\
&= \frac{M}{2} \left[\dot{q}^2 - \Omega_f^2(t) q^2 \right]
\end{aligned} \tag{31}$$

where $\Omega_f(t) \equiv (1+f)^{1/2} \Omega(t)$.

It is but natural that the scale factor cannot take the same value when inhomogeneity is present. Technically this means that *now it has to be some different function of the time t* . To distinguish these two cases, i.e. homogeneous and inhomogeneous, we write the scale factor in the presence of inhomogeneity as $a_f(t)$ instead of $a(t)$ which denotes the homogeneous scenario. In the same spirit, the functions ν_f, ψ_f, ξ_f are also different functions of time from their homogeneous counterparts, *viz.*, ν, ψ and ξ .

To estimate quantum fluctuations of the temperature in the presence of inhomogeneity (f), we first assert that the dynamical variable $q(t) = \ln a(t)$ will be modified in presence of inhomogeneity which we denote by the notation $q_f(t) = \ln a_f(t)$. Then we write this as $q_f(t) = q_{f,\text{cl}}(t) + y_f(t)$ where $y_f(t)$ ($0 < y_f(t) < \infty$) is the fluctuation over the classical value $q_{f,\text{cl}}(t)$. We take $q_{f,\text{cl}} = q_{\text{cl}}$, so that $q_f(t) = q_{\text{cl}}(t) + y_f(t)$ and $y_f(t)$ gives the fluctuation (in presence of inhomogeneity) over the same classical value q_{cl} . Then the quantum mechanical amplitude for q_f to evolve from a value $q_{fa}(t_a)$ to $q_{fb}(t_b)$ is given by

$$\langle q_{fa}, t_a | q_{fb}, t_b \rangle = F_f(t_b, t_a) \exp \left(\frac{i}{\hbar} S_{f,\text{cl}} \right) \tag{32}$$

where $S_{f,\text{cl}} = \int L_{f,\text{cl}} dt = \int_{t_a}^{t_b} \frac{M}{2} \left[\dot{q}_{\text{cl}}^2 - \Omega_f^2(t) q_{\text{cl}}^2 \right]$ which is structurally same as S_{cl} but with Ω replaced by Ω_f ; and the fluctuation factor $F_f(t_a, t_b)$ can again be calculated following [28]. The fluctuations $y_f(t)$ now satisfies the differential equation

$$\ddot{y}_f + \Omega_f^2(t) y_f = 0. \tag{33}$$

As before, two independent quasi-periodic solutions of Eq. (33) (for real Ω_f) can be considered as

$$y_{f1}(t) = \Psi_f(t) \sin \xi_f(t, t_a) \quad , \quad y_{f2}(t) = \Psi_f(t) \sin \xi_f(t_b, t) \tag{34}$$

with boundary conditions

$$y_{f1}(t_a) = 0 \quad ; \quad y_{f2}(t_b) = 0 \tag{35}$$

where, $\Psi_f(t)$ satisfies the Ermakov-Pinney equation

$$\ddot{\Psi}_f + \Omega_f^2(t) \Psi_f - \Psi_f^{-3} = 0 \tag{36}$$

with $\xi_f(t, s)$ defined as

$$\xi_f(t, s) \equiv \nu_f(t) - \nu_f(s) = \int_s^t \Psi_f^{-2}(t') dt' \tag{37}$$

Here $\Psi_f(t)$ and $\nu_f(t)$ respectively represent the amplitude and phase of the time dependent oscillator. The fluctuation factor $F_f(t_b, t_a)$ in presence of inhomogeneity is then given by

$$F_f(t_b, t_a) = \left[\frac{M \sqrt{(\dot{\nu}_f)_a (\dot{\nu}_f)_b}}{2\pi i \hbar \sin \xi_f(t_b, t_a)} \right]^{1/2} \quad (38)$$

So the amplitude is (for relevant boundary conditions $q_f(t_a) = q_{fa}, q_f(t_b) = q_{fb}$),

$$\langle q_{fb}, t_{fb} | q_{fa}, t_{fa} \rangle = \left[\frac{M \sqrt{(\dot{\nu}_f)_a (\dot{\nu}_f)_b}}{2\pi i \hbar \sin \xi_f(t_b, t_a)} \right]^{1/2} \left[\exp \left(\frac{i S_{f,cl}^+}{\hbar} \right) - \exp \left(\frac{i S_{f,cl}^-}{\hbar} \right) \right] \quad (39)$$

where

$$S_{f,cl}^\pm = \left(\frac{\dot{\Psi}_{fb} q_{fb}^2}{\Psi_{fb}} - \frac{\dot{\Psi}_{fa} q_{fa}^2}{\Psi_{fa}} \right) + \frac{1}{\sin \xi_f(t_b, t_a)} \left[(\dot{\nu}_{fb} q_{fb}^2 + \dot{\nu}_{fa} q_{fa}^2) \cos \xi_f(t_b, t_a) \mp 2 \sqrt{\dot{\nu}_{fb} \dot{\nu}_{fa}} q_{fb} q_{fa} \right] \quad (40)$$

For small $\dot{\nu}_f \ll 1$, to lowest order in $\dot{\nu}$, the probability of transition for logarithm of scale factor (inverse temperature) in presence of inhomogeneity would be

$$P_f(b, a) = |\langle q_{fa}, t_{fa} | q_{fb}, t_{fb} \rangle|^2 = \frac{3m_{pl}^2}{\pi^2} (\ln T_{fa})^2 (\ln T_{fb})^2 \frac{(\dot{\nu}_{fa} \dot{\nu}_{fb})^{3/2}}{\sin^3 \xi_f(t_b, t_a)} \quad (41)$$

We now choose to write

$$\Psi_f(t) = (1 + f) \psi(t) \quad (42)$$

so that for $f = 0$, $\Psi_f(t) \rightarrow \psi(t)$ and $\Omega_f(t) \rightarrow \Omega(t)$ and we get back homogeneous scenario. Also for such a choice the quantities ν_f and ξ_f appearing in Eq. (41) can be expressed explicitly in terms of respective quantities ν and ξ corresponding to the homogeneous scenario in manner described below.

If we choose $e^{\gamma_f(t)}$ to represent a solution of the Ermakov-Pinney equation [Eq. (36)], then in order the Eq. (42) is satisfied, $\gamma_f(t)$ will be related to the parameter γ (recall that: $e^{\gamma t}$ represents a solution of the Ermakov-Pinney equation (Eq. (13)) corresponding to the homogeneous case) by the following relation

$$\gamma_f(t) = \gamma t + \ln(1 + f) \quad (43)$$

Note here that the way we choose to incorporate the inhomogeneity into our scheme retains the Ermakov-Pinney structure of the differential equations which is the central feature of the formalism described in Sec. 2. This will ensure that new solutions thereby obtained will obey all the mathematical properties of Ermakov theory regarding the form of the nonlinear equations.

It is quite evident that Ψ reduces to $\psi(t)$ if $f = 0$ and then $\gamma_f(t)$ reduces to γt and we get back the original situation. Therefore we can unambiguously use the previous formalism with $P(b, a)$ replaced by $P_f(b, a)$, $\nu(t)$'s replaced by $\nu_f(t)$'s and $\xi(t_b, t_a)$ replaced by $\xi_f(t_b, t_a)$ respectively. Now with $\Psi_f(t) =$

$e^{\gamma_f(t)}$ the new $\nu_f(t)$ and $\xi_f(t_b, t_a)$ are related to corresponding functions for homogeneous case by the following relations

$$\nu_f(t) = \frac{\nu(t)}{[1+f]^2} \quad (44)$$

$$\xi_f(t_b, t_a) = \nu_f(t_b) - \nu_f(t_a) = \frac{\nu(t_b) - \nu(t_a)}{[1+f]^2} \quad (45)$$

Using Eqs. (44) and (45) in Eq. (41) we get

$$P_f(b, a) = \frac{3m_{\text{pl}}^2}{\pi^2} (\ln T_a)^2 (\ln T_b)^2 \left[p_{0f}(b, a) + p_{1f}(b, a) + p_{2f}(b, a) + \dots \right] \quad (46)$$

where the quantities $p_{0f}, p_{1f}, p_{2f}, \dots$ appearing in the above equation is expressible in terms of their homogeneous counterparts as

$$\begin{aligned} p_{0f}(b, a) &= \frac{[\dot{\nu}_f(t_a)\dot{\nu}_f(t_b)]^{3/2}}{\xi_f^3(t_b, t_a)} = \frac{[\dot{\nu}(t_a)\dot{\nu}(t_b)]^{3/2}/(1+f)^6}{\xi^3(t_b, t_a)/(1+f)^6} \\ &= p_0(b, a) \\ p_{1f}(b, a) &= \frac{1}{2} \frac{[\dot{\nu}_f(t_a)\dot{\nu}_f(t_b)]^{3/2}}{\xi_f^3(t_b, t_a)} = \frac{1}{2} \frac{[\dot{\nu}(t_a)\dot{\nu}(t_b)]^{3/2}/(1+f)^6}{\xi^3(t_b, t_a)/(1+f)^6} \\ &= \frac{p_1(b, a)}{(1+f)^4} = p_1(b, a)(1 - 4f + \mathcal{O}(f^2)) \\ p_{2f}(b, a) &= \frac{17}{120} [\dot{\nu}_f(t_a)\dot{\nu}_f(t_b)]^{3/2} \xi_f(t_b, t_a) \\ &= \frac{p_2(b, a)}{(1+f)^8} = p_2(b, a)(1 - 8f + \mathcal{O}(f^2)) \\ &\vdots \\ p_{nf}(b, a) &= \frac{p_n(b, a)}{(1+f)^{4n}} = p_n(b, a)(1 - 4nf + \mathcal{O}(f^2)) \end{aligned}$$

In terms of γ, t_a and t_b the above expression becomes

$$\begin{aligned} P_f(b, a) &= \frac{3m_{\text{pl}}^2}{\pi^2} (\ln T_a)^2 (\ln T_b)^2 \times \\ &\quad \left[\frac{1}{(t_b - t_a)^3} \left[1 - \frac{1}{2}(t_b - t_a)^2 \gamma^2 + \dots \right] \right. \\ &\quad + \frac{1}{2(t_b - t_a)(1+f)^4} \left[1 - 2(t_b + t_a)\gamma + \frac{1}{6}(11t_b^2 + 11t_a^2 + 26t_b t_a)\gamma^2 + \dots \right] \\ &\quad \left. + \frac{17}{120} \frac{(t_b - t_a)}{(1+f)^8} \left[1 - 4(t_b + t_a)\gamma + \frac{1}{6}(49t_b^2 + 49t_a^2 + 94t_b t_a)\gamma^2 + \dots \right] \right] \quad (47) \end{aligned}$$

3 Extracting time dependence of scale factor from observational data

Measurement of luminosity distance of the type Ia Supernovae (SNe Ia) during nearly last two decades establishes that the universe is presently undergoing a phase of accelerated expansion. Observation of

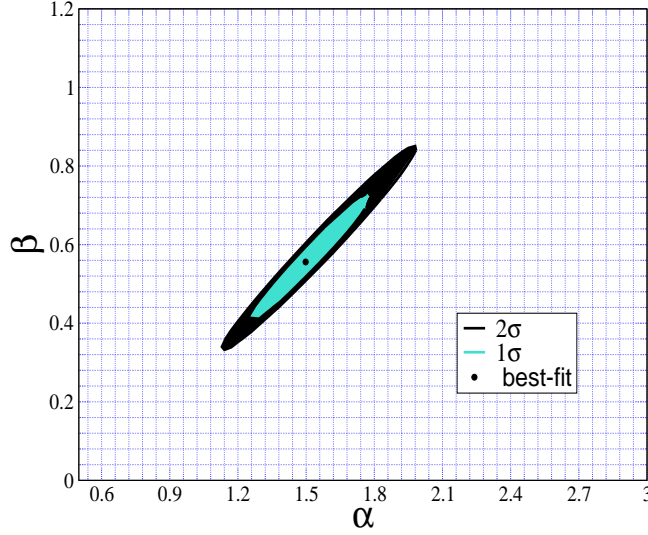


Figure 1: Allowed regions in the parameter space $\alpha - \beta$ at 1σ and 2σ confidence level from the combined analysis of SNe Ia data and OHD

Baryon Acoustic Oscillations (BAO), Cosmic Microwave Background (CMB) radiations, power spectrum of matter distributions in the universe provide other independent evidence in favour of this late-time cosmic acceleration. However, the SNe Ia data remain the key observational ingredient in determining time evolution of the scale factor $a(t)$ in the late-time phase of evolution of the universe. Besides the SNe Ia data, observational data based on measurement of differential ages of the galaxies by Gemini Deep Deep Survey GDDS [8], SPICES and VDSS surveys also provide dependence of Hubble parameter with redshift. We have extracted the this time evolution from the combined analysis of SNe Ia data and observational Hubble data.

3.1 Methodology of analysis of SNe Ia and Observational Hubble data

Here we briefly describe the methodology we use for the combined analysis of SNe Ia and Observational Hubble Data (OHD). We use a closed form parametrisation of the luminosity distance of supernova, d_L , as a function of the redshift as [13]

$$d_L(\alpha, \beta, z) = \frac{c}{H_0} \left(\frac{z(1 + \alpha z)}{1 + \beta z} \right) \quad (48)$$

where c is the speed of light and H_0 the value of the Hubble parameter at the present epoch defined through the dimensionless quantity h by $H_0 = 100 h \text{ km s}^{-1} \text{ Mpc}^{-1}$. The luminosity distance is related to the distance modulus μ as

$$\begin{aligned} \mu_{\text{th}}(\alpha, \beta, z) &= 5 \log_{10} \left[D_L(\alpha, \beta, z) \right] + \mu_0 \\ &= 5 \log_{10} \left[\left(\frac{z(1 + \alpha z)}{1 + \beta z} \right) \right] + \mu_0 \end{aligned} \quad (49)$$

where,

$$D_L(\alpha, \beta, z) \equiv \frac{H_0}{c} d_L(\alpha, \beta, z) = \left(\frac{z(1 + \alpha z)}{1 + \beta z} \right) \quad (50)$$

is a dimensionless quantity called the Hubble free luminosity distance and $\mu_0 = 42.38 - 5 \log_{10} h$. From different compilations of SNe Ia observations by different groups - HST + SNLS + ESSENCE [1, 2, 3], SALT2 and MLCS data [4], UNION [5] and UNION2 data [6]. provide the values of the distance modulus for different values of the redshift from the SNe Ia observations. The observed values of the distance modulus $\mu_{\text{obs}}(z_i)$ corresponding to measured redshifts z_i are given in terms of the absolute magnitude M and the apparent magnitudes $m_{\text{obs}}(z_i)$ by

$$\mu_{\text{obs}}(z_i) = m_{\text{obs}}(z_i) - M. \quad (51)$$

To obtain the best-fit values of the parameters α and β from SNe Ia observations we perform a likelihood analysis whose methodology has been discussed in detail in [7]. This involves minimization of a suitably chosen χ^2 function with respect to the parameters α and β . We give below a brief outline of the methodology of χ^2 -analysis adopted here for the analysis of SNe Ia data. The χ^2 function is defined as the function of the parameters α , β and $M' \equiv \mu_0 + M$ (called nuisance parameter) as

$$\begin{aligned} \chi^2(\alpha, \beta, M') &= \sum_{i=1}^N \frac{(\mu_{\text{obs}}(z_i) - \mu_{\text{th}}(\alpha, \beta, z_i))^2}{\sigma_i^2} \\ &= \sum_{i=1}^N \frac{[5 \log_{10} D_L(\alpha, \beta, z_i) - m_{\text{obs}}(z_i) + M']^2}{\sigma_i^2} \end{aligned} \quad (52)$$

where σ_i 's are the uncertainties in observations of distance modulus $\mu_{\text{obs}}(z_i)$'s, and N is the total number of data points. The values of the parameters α and β (appearing in parametrisation of luminosity distance) which fits the SNe IA data best, are those which minimizes the χ^2 function after the parameter M' is marginalised over. Expanding the χ^2 function as

$$\chi^2 = P(\alpha, \beta) + 2Q(\alpha, \beta)M' + RM'^2 \quad (53)$$

where

$$P(\alpha, \beta) = \sum_{i=1}^N \frac{(5 \log_{10}(D_L(\alpha, \beta, z_i)) - m_{\text{obs}}(z_i))^2}{\sigma_i^2} \quad (54)$$

$$Q(\alpha, \beta) = \sum_{i=1}^N \frac{(5 \log_{10}(D_L(\alpha, \beta, z_i)) - m_{\text{obs}}(z_i))}{\sigma_i^2} \quad (55)$$

$$R = \sum_{i=1}^N \frac{1}{\sigma_i^2} \quad (56)$$

we observe that, the χ^2 have a minimum at $M' = -Q/R$ and its value at the minimum is $\bar{\chi}^2(\alpha, \beta) = P - Q^2/R$. To obtain the best-fit value of the parameters α and β its then enough to minimize the

function $\bar{\chi}^2(\alpha, \beta)$ with respect to α and β only since the effect of marginalisation over M' gets taken care of in the above consideration. So the χ^2 -function for analysis of SNe Ia data used here is

$$\chi_{\text{SN}}^2(\alpha, \beta) = P(\alpha, \beta) - \frac{Q^2(\alpha, \beta)}{R} \quad (57)$$

where $P(\alpha, \beta)$, $Q(\alpha, \beta)$ and R are given by Eqs. (54), (55) and (56) respectively.

Besides the SNe Ia data, compilation of the observational data based on measurement of differential ages of the galaxies by Gemini Deep Deep Survey GDDS [8], SPICES and VDSS surveys provide the values of the Hubble parameter at 15 different redshift values [9, 10, 11, 12]. The χ^2 function for the analysis of this observational Hubble data can be defined as

$$\chi_{\text{OHD}}^2(\alpha, \beta) = \sum_{i=1}^{15} \left[\frac{H(\alpha, \beta; z_i) - H_{\text{obs}}(z_i)}{\Sigma_i} \right]^2, \quad (58)$$

where H_{obs} is the observed Hubble parameter value at z_i with uncertainty Σ_i .

Varying the parameters α and β freely we minimize the global χ^2 function which is defined as

$$\chi^2(\alpha, \beta) = \chi_{\text{SN}}^2(\alpha, \beta) + \chi_{\text{OHD}}^2(\alpha, \beta). \quad (59)$$

The values of the parameters α and β at which minimum of χ^2 is obtained are the best-fit values of these parameters for the combined analysis of the observational data from SNe Ia and Observational Hubble Data (OHD). We also find the 1σ and 2σ ranges of the parameters α and β from the analysis of the observational data discussed above. In this case of two parameter fit, the 1σ (68.3% confidence level) and 2σ (95.4% confidence level) allowed ranges of the parameters correspond to $\chi^2 \leq \chi_{\text{min}}^2 + \Delta\chi^2$, where $\Delta\chi^2 = 2.30(6.17)$ denotes the $1\sigma(2\sigma)$ spread in χ^2 corresponding to two parameter fit.

In this work we have considered the SNe Ia data from HST+SNLS+ESSENCE (192 data points) [1, 2, 3] and Observational Hubble Data from [9, 10, 11, 12] (15 data points). The best fit for the combined analysis of the SNe Ia data and OHD is obtained for the parameters values

$$\alpha = 1.50 \quad , \quad \beta = 0.55 \quad (60)$$

with a minimum χ^2 of 204.94. In Fig. 1 we have shown the regions of the $\alpha - \beta$ parameter space allowed at 1σ and 2σ confidence levels from the analysis.

3.2 Methodology of obtaining time dependence of scale factor from observational data

Using the values of α and β (Eq. (60)) as obtained from the analysis we can determine the time dependence of the scale factor and the Hubble parameter during the late time evolution of the universe.

For a flat universe, which is consistent with the current bounds from PLANCK and WMAP data on the ratio of the energy density in curvature to the critical density, $|\Omega_K^0| < 0.01$ (95% confidence level) (PLANCK) the Hubble parameter $H(z)$ corresponding to a redshift z is directly related to the luminosity distance through the relation

$$E(z) \equiv \frac{H(z)}{H_0} = \left[\frac{d}{dz} \left(\frac{D_L(z)}{1+z} \right) \right]^{-1} \quad (61)$$

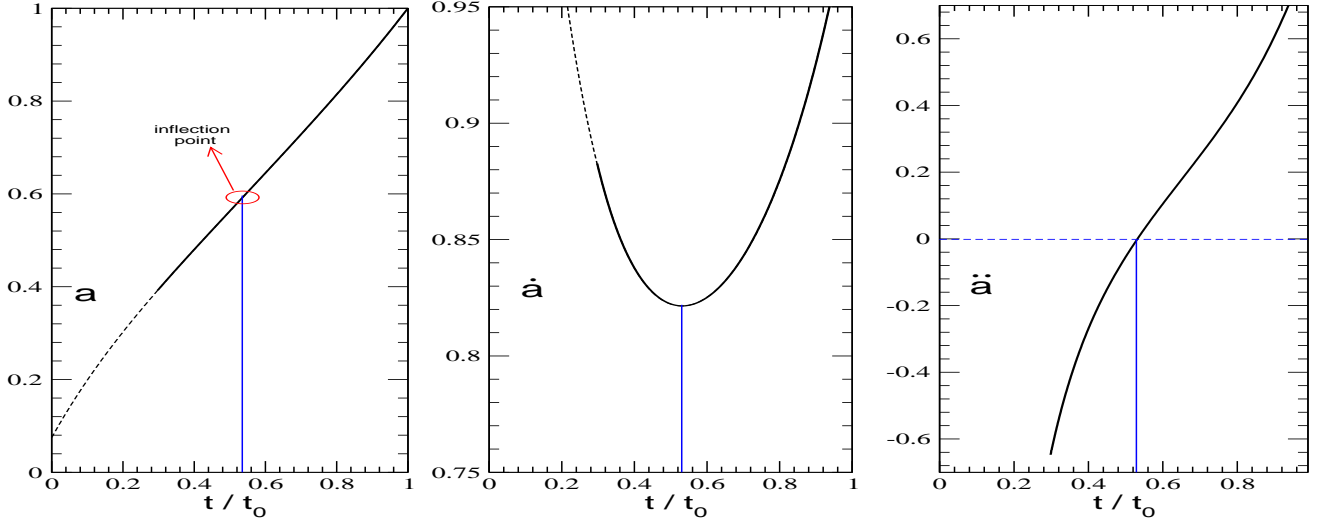


Figure 2: Plot of a (left panel), \dot{a} (middle panel) and \ddot{a} (right panel) against t corresponding to the best-fit values of parameters α and β obtained from analysis of SN data.

From the equations $H = \frac{\dot{a}}{a}$ and $\frac{a_0}{a} = 1 + z$ we get

$$dt = -\frac{dz}{(1+z)H} = -\frac{dz}{(1+z)H_0 E(z)} \quad (62)$$

which on integration gives

$$\frac{t(z)}{t_0} = 1 - \frac{1}{H_0 t_0} \int_z^0 \frac{dz'}{(1+z')E(z')} \quad (63)$$

where t_0 is the time corresponding to present epoch. Taking the best-fit values of α and β , we use Eq. (50) to numerically evaluate $D_L(z)$ at different z values. Using this in Eq. (61) we then evaluate $E(z)$ as a function of z which can further be used in Eq. (63) to perform the integration numerically to obtain time t as a function of redshift z . From the $z - t(z)$ relationship thus obtained and the equation $a_0/a = 1 + z$ we eliminate z to obtain the scale factor a as a function of t .

In Fig. (2) we have shown the time dependence of the scale factor as obtained from the analysis of the observational data following technique described above. The left panel shows plot of $a(t)$ vs t/t_0 where the value of scale factor at present epoch has been normalised to unity $a(t_0) = 1$. The observed supernova Ia events have redshifts ranging between $0 < z \lesssim 1.6$ which correspond to the range $0.3 \lesssim t/t_0 < 1$. In the obtained t -dependence of $a(t)$ there exists a point of inflection at $t/t_0 \approx 0.53$ ($z \approx 0.68$). This feature transforms into a minimum in the middle panel where we have plotted \dot{a} against t . In the right panel (\ddot{a} vs t) again there is the signature of crossover to an accelerated phase of expansion.

4 Results and discussions

We now investigate various aspects of the transition probability (Eq. (47)) and implications of its dependences on the two parameters of the theory - γ (appearing in the solution of Ermakov-Pinney

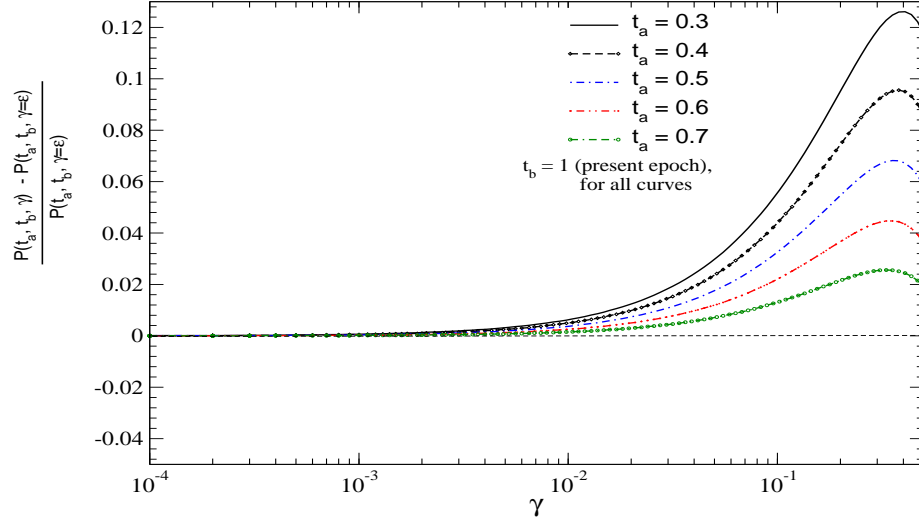


Figure 3: Plot of $[P_\gamma(t_a, t_b) - P_{\gamma=\epsilon}(t_a, t_b)]/P_{\gamma=\epsilon}(t_a, t_b)$ vs γ for $t_b = 1$ (present epoch) and for different chosen values of t_a . We take $\epsilon = 10^{-6}$.

equation) and f (phenomenological parameter as a measure inhomogeneity), as well as the epochs (t_a, t_b) between which the transition is considered. To calculate the transition probability, we use the fact microwave background temperature at time t , $T(t) \propto \frac{1}{a(t)}$ and we make use of time dependence of $a(t)$ as obtained from the combined analysis of SNe Ia and observational Hubble data described in Sec. 3.

To find the γ sensitivity of the theory we investigate the γ -dependence of the the quantity $\mathcal{P}(\gamma)$ defined as

$$\mathcal{P}(\gamma) \equiv \frac{P_\gamma(t_b, t_a) - P_{\gamma=\epsilon}(t_b, t_a)}{P_{\gamma=\epsilon}(t_b, t_a)} \quad (64)$$

where we take $\epsilon = 10^{-6}$. For a given t_a, t_b the quantity $\mathcal{P}(\gamma)$ is a measure of fractional change in the transition probability due to variation of the parameter γ from the arbitrarily chosen small value 10^{-6} . In figure (3) we plot $\mathcal{P}(\gamma)$ vs γ , for fixed values of t_a, t_b and taking $f = 0$. For all the plots we have kept fixed $t_b = 1$ (present epoch) and have shown the plots for different chosen values of t_a . We see from the figure that for small γ , viz. $\gamma < 0.01$, \mathcal{P} remains effectively same for all epochs implying that basic results of the model are insensitive to the values of γ .

The dependence of the transition probability on the epochs t_a and t_b , between which the transition has been considered is shown in Fig. 4 where we plot $P_\gamma(t_a, t_b, f)$ against t_a for three chosen values of the phenomenological parameter f viz. 0, 0.2 and 0.6. We have taken $\gamma = 10^{-6}$ for the plots, but the plots will remain same for all values of $\gamma < 0.01$ as already seen from results presented in Fig. 3.

The plots of Fig. 4 show that the probability of transition from an epoch t to the present epoch $t = 1$ falls slowly with t in the decelerated phase of expansion of the universe. It attains a minimum at a value of t near $t \approx 0.5$ which is almost the same epoch where the expansion of universe enters the accelerated phase from decelerated phase. The probability starts increasing with t in the accelerated phase of expansion and rises sharply with t as it approaches more towards the present epoch. So the nature of t -dependence of the probability $P(t, t = 1)$ has a profile similar to that of \dot{a} , as evident from the middle panel of Fig. 2.

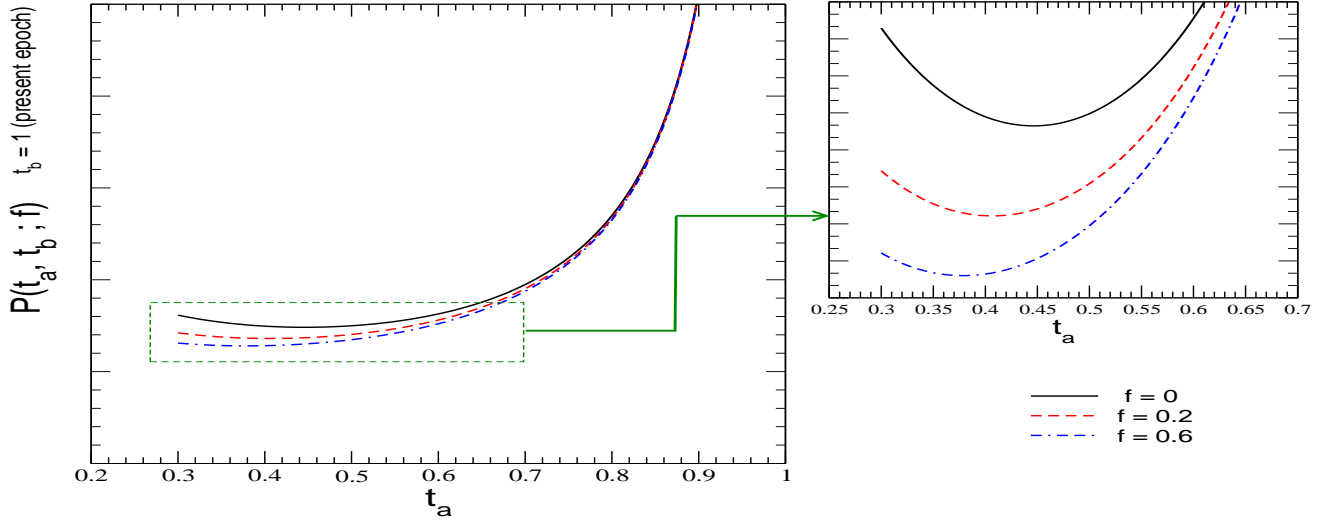


Figure 4: Plot of $P(t_a, t_b, f)$ vs t_a for $t_b = 1$ (present epoch) for the homogeneous case and two non-zero benchmark values of inhomogeneity parameter f

The nature of the Fig. 4 is further corroborated by an interesting plot. In the left panel of Fig. 5 the solid line is the plot of $P(t_a, t_b = 1)$ vs t_a with the t -dependence of $a(t)$ taken as $a(t) \sim t^{2/3}$ for all epochs. This corresponds to a decelerated expansion of the universe dominated by matter. The dotted line is the plot of $P(t_a, t_b = 1)$ vs t_a with the t -dependence of $a(t)$ as $a(t) \sim e^{Ht}$ for all epochs. This corresponds to a dark energy driven accelerated expansion of universe. The t_a -dependence of $P(t_a, t_b = 1)$ obtained in the theory is given by Eq. (47). The t_a dependence enters in the probability through a multiplicative term $(\ln T_a)^2 \sim (\ln a(t_a))^2 \equiv \eta_1$ (say), and through the term in the square bracket η_2 , say. For low values of γ used in our computation, the term η_2 increases with t_a as t_a approaches the present epoch ($t_b = 1$), while the term η_1 goes as $(\ln t_a)^2$ for $a \sim t^{2/3}$ (matter dominated universe) and as t_a^2 for $a \sim e^{Ht}$ (dark energy dominated universe). Since the time parameter t we use is normalised to 1 at present epoch, t_a is fractional, and $(\ln t_a)^2$ decreases as t_a approaches $t_b = 1$, while t_a^2 always increases with t_a in the domain under consideration. The fact that the probability is a product of η_1 and η_2 , there is a resultant behaviour which determines the turning point (minimum) at $t_a \sim 0.5$ after which the contribution from η_2 dominates and we are in the accelerated phase.

In the right panel of Fig. 5 we plot $P(t_a, t_b = 1)$ vs t_a with $a(t) \sim t^{2/3}$ up till $t_a \sim 0.5$. That is, the behaviour of $a(t)$ is taken to be that of a matter dominated universe. After $t_a \sim 0.5$ we take the behaviour of $a(t) \sim e^{Ht}$ and compute $P(t_a, t_b = 1)$. Here we are taking a dark energy dominated scenario. Note that the graph mimics Fig. 4 to a great extent except for a discontinuous portion around $t_a \sim 0.5$. This is expected as the change over from a decelerating to an accelerated phase is bound to be associated with a discontinuity which cannot be analytically obtained from a phenomenological model. Mathematically also this is expected because there cannot be a smooth transition from $t^{2/3}$ behaviour to that of e^{Ht} . However the overall behaviour (*i.e.* a transition from decelerating to an accelerating phase) is reflected in the graphical transcription.

From Fig. 4 we also get a qualitative indication how the presence of inhomogeneity affects the evolution of transition probability between different temperatures. This is shown more comprehensively in Fig. 6 where we have again plotted $P(t_a, t_b = 1)$ vs t_a (left panel) for different values of f , both positive and negative. For comparison we have also shown the plot of $\dot{a}(t)$ vs t obtained from analysis

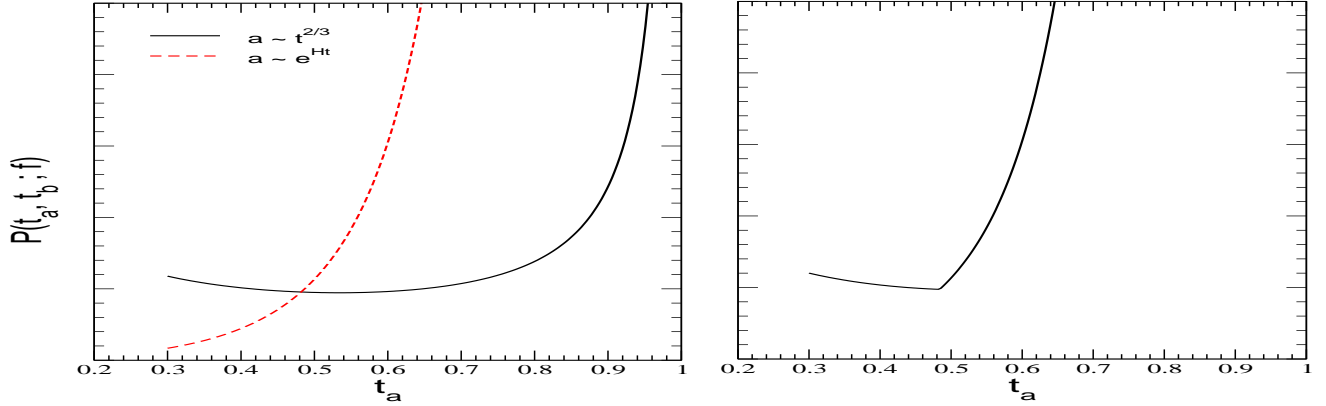


Figure 5: Left panel: Plot of $P(t_a, t_b)$ vs t_a for $t_b = 1$ (present epoch) for the homogeneous case with $a(t) \sim t^{2/3}$ for all all epochs (solid line) and with $a(t) \sim e^{Ht}$ for all epochs (dotted line). Right panel: Plot of $P(t_a, t_b)$ vs t_a for $t_b = 1$ (present epoch) for the homogeneous case with $a(t) \sim t^{2/3}$ for $t < 0.5$ and with $a(t) \sim e^{Ht}$ for $t > 0.5$.

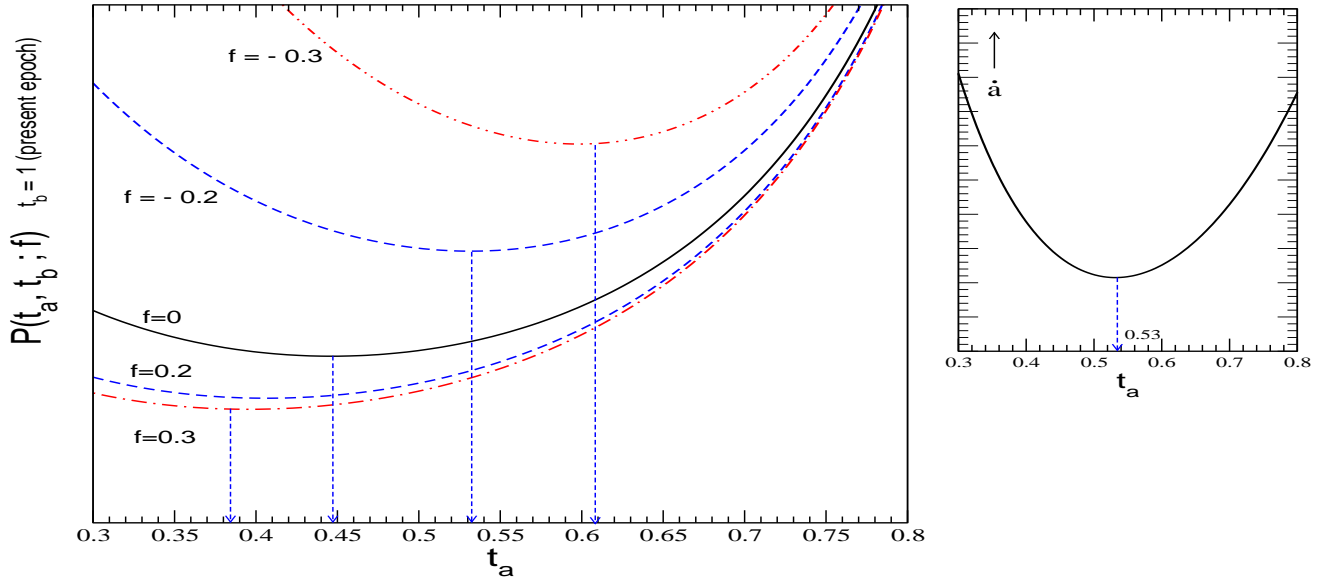


Figure 6: Left panel: Plot of $P(t_a, t_b)$ vs t_a for $t_b = 1$ (present epoch) for the different values of f , Right panel : Plot of $\dot{a}(t)$ vs t obtained from analysis of observational data.

of observational data in the right panel. Fig. 6 shows that the probability is sensitive to the presence of inhomogeneity. This sensitivity increases as one goes further into the past and larger absolute value of the inhomogeneity parameter, $|f|$, leads to larger departure from probability values corresponding to the homogeneous scenario. Also the value of the inhomogeneity parameter determines the epoch of switch over from a decelerated to an accelerated phase of expansion of the universe. A positive value leads to switch over at earlier epochs, while a negative value leads to switch over at later epochs. We obtain better agreement with the observed value of crossover point $t \approx 0.53$ for a negative value of

inhomogeneity parameter $f \approx -0.2$.

5 Conclusion

In this work a phenomenological model has been developed to study the evolution of the universe in the context of the CMBR. A key ingredient of the model is the presence of dark energy through a scalar field whose kinetic energy dominates i.e. a k -essence scalar field. We first develop the observational evidence through a rigorous graphical transcription of SNe Ia data. This is depicted in Fig. 2. Subsequently a Lagrangian model of dark energy (obtained from very general considerations, Sec. 2) is used to explain the evidence depicted in Fig. 2.

The approach taken is as follows. The Lagrangian (Eq. (8)) is that of a time dependent oscillator and the dynamical variables is $q = \ln a(t)$. We compute the quantum fluctuations $\langle q_a, t_a | q_b, t_b \rangle$ which is tantamount to computing the correlations between the logarithm of the temperatures at two epochs t_a and t_b where we have used the association between the scale factor $a(t)$ and cosmic temperature at a particular epoch, viz., $T_a \sim \frac{1}{a(t_a)}$.

What is remarkable is that the probability of transition between the logarithm of the temperatures $\ln T_a$ at $t = t_a$ and $\ln T_b$ at $t = t_b$ (present epoch) follows a similar profile as that of $\dot{a}(t)$. This is shown in Fig. 4. Another point of note is that the crossover from a decelerating phase to an accelerated phase occurs at precisely at the same epoch, viz., i.e. $t_a = 0.5$.

This shows that our model captures the essential physics because the probability seems to be proportional to $\dot{a}(t)$ and as $a(t + dt) \sim a(t) + \dot{a}(t)dt$, therefore the probability of transition should be proportional to \dot{a} . Figs. 2 and 4 seem to confirm this fact.

Our phenomenological model successfully explains the observed variation of \dot{a} . This conclusion follows from the fact that the variation of \dot{a} matches with the probability profile obtained theoretically from the model after plugging in observed values of \dot{a} at corresponding epochs. Moreover, the observed value of the epoch when the universe went from a decelerating phase to an accelerated phase, it is nearly the same as that obtained from the theoretically obtained profile.

This model also throws light on how inhomogeneity may affect the CMBR evolution. There is a qualitative indication that the probability is sensitive to the presence of inhomogeneity and this sensitivity increases as one goes further into the past. Also the value of the inhomogeneity parameter determines the epoch of switch over to an accelerated phase. A positive value leads to switch over at earlier epochs, while a negative value leads to switch over at later epochs. Better agreement with the observed value of crossover point is obtained for a small negative value of the inhomogeneity parameter. This is seen from Fig. 6.

References

- [1] A. G. Riess et al., *Astrophys. J.* 659, 98 (2007)
- [2] W. M. Wood-Vasey et al., *Astrophys. J.* 666, 694 (2007)
- [3] T. M. Davis et al., *Astrophys. J.* 666, 716 (2007)
- [4] R. Kessler et al., *Astrophys. J. Suppl.* 185 , 32 (2009)
- [5] M. Kowalski et al. *Astrophys. J.* 686, 749 (2008)

- [6] R. Amanullah et al., *Astrophys. J.* 716, 712 (2010)
- [7] L. Xu, Y. Wang, *JCAP* 1006, 002 (2010), S. Nesseris and L. Perivolaropoulos, *Phys. Rev. D* **72** 123519 (2005); L. Perivolaropoulos, *Phys. Rev. D* **71** 063503 (2005); E. Di Pietro and J. F. Claeskens, *Mon. Not. Roy. Astron. Soc.* **341** 1299 (2003); A. C. C. Guimaraes, J. V. Cunha and J. A. S. Lima, *JCAP* **0910** 010 (2009).
- [8] R. G. Abraham et al., *Astron. J.* 127, 2455 (2004)
- [9] J. Simon, L. Verde and R. Jimenez, *Phys. Rev. D* 71, 123001 (2005)
- [10] E. Gaztanaga, A. Cabre, L. Hui, *Mon. Not. Roy. Astron. Soc.* 399, 166 (2009)
- [11] A. G. Riess et al., *Astrophys. J.* 699, 539 (2009)
- [12] D. Stern, R. Jimenez, L. Verde, M. Kamionkausk, S. A. .Stanford, *JCAP* 1002, 008 (2010)
- [13] T. Padmanabhan and T. R. Choudhury, *Mon. Not. Roy. Astron. Soc.* 344, 823 (2003)
- [14] E. Komatsu *et al.*, *Astrophys. J. Suppl.* **192**, 18 (2011)
- [15] P. A. R. Ade *et al.* [Planck Collaboration], arXiv:1303.5062 [astro-ph.CO]. P. A. R. Ade *et al.* [Planck Collaboration], arXiv:1303.5072 [astro-ph.CO]. P. A. R. Ade *et al.* [Planck Collaboration], arXiv:1303.5075 [astro-ph.CO].
- [16] S. Cole *et al.* *Mon. Not. Roy. Astron. Soc.* **362**, 505 (2005)
- [17] G. Huetsi, *Astron. Astrophys.* **449**, 891 (2006)
- [18] W. J. Percival *et al.*, *Astrophys. J.* **657**, 51 (2007)
- [19] D. Eisenstein, *Astrophys. J.*, **633**, 560 (2005)
- [20] V.Sahni, Dark matter and dark energy, *Lect.Notes Phys.* 653 141 (2004) [astro-ph/0403324]; 843 111 (2006)[astro-ph/0602117]; T.Padmanabhan, Dark energy: mystery of the millenium, *AIP Conf.Proc.* 861 179 (2006) [astro-ph/0603114]; T.Padmanabhan, Dark energy and gravity, *Gen.Rel.Grav.* 40 529 (2007) [arXiv:0705.2533]; E.J.Copeland, M.Sami and S.Tsujikawa, Dynamics of dark energy, *Int.Jour.Mod.Phys. D15* 1753 (2006) [hep-th/0603057].
- [21] P.J.E.Peebles and B.Ratra, The cosmological constant and dark energy, *Rev.Mod.Phys.* 75 559 (2003) ; T.Padmanabhan, Cosmological constant-the weight of the vacuum, *Physics Reports* 380 235 (2003) [hep-th/0212290].
- [22] M.Malquarti, E.J.Copeland, A.R.Liddle and M.Trodden, A new view of k-essence, *Phys.Rev. D* 67 123503 (2003) [astro-ph/0302279] M.Malquarti, E.J.Copeland and A.R.Liddle, K-essence and the coincidence problem, *Phys.Rev. D* 68 023512 (2003) [astro-ph/0304277]; L.Mingzhe and X.Zhang, K-essence leptogenesis, *Phys.Lett. B* 573 20 (2003) [hep-ph/0209093]; J.M.Aguirregabiria, L.P.Chimento and R.Lazkoz, Phantom k-essence cosmologies, *Phys.Rev. D* 70 023509 (2004) [astro-ph/0403157].

- [23] L.P.Chimento and R.Lazkoz,Phys.Rev. D71 023505 (2005); L.P.Chimento,M.Forte and R.Lazkoz, Mod.Phys.Lett. A20 2075 (2005); R.Lazkoz,Int.Jour.Mod.Phys. D14 635 (2005) [gr-qc/0410019]; H.Kim, Phys.Lett. B606 223 (2005); J.M.Aguirregabiria,L.P.Chimento and R.Lazkoz, Phys.Lett. B631 93 (2005); H.Wei and R.G.Cai,Phys.Rev. D71 043504 (2005) [hep-th/0412045]; C.Armendariz-Picon and E.A.Lim, JCAP 0508 7 (2005).
- [24] L.R.Abramo and N.Pinto-Neto,Phys.Rev. D73 063522 (2006); A.D.Rendall,Class.Quant.Grav.**23** 1557 (2006) [gr-qc/0511158].
- [25] D. Gangopadhyay and S. Mukherjee,Phys. Lett. B **665**, 121 (2008)
- [26] R.J.Scherrer, Phys.Rev.Lett **93** 011301(2004) L.P.Chimento,Phys.Rev. D69 123517 (2004)
- [27] D. Gangopadhyay, Gravitation and Cosmology **16**, 231 (2010)
- [28] D.C.Khandekar and S.V.Lawande,Phys.Rep.**137** 115 (1986).
- [29] H.Ezawa,J.R.Klauder and L.A.Shepp, J.Math.Phys. **16** 783 (1975).
- [30] B.Simon, J.Functional Analysis and Applications **14** 295 (1973).
- [31] T.E.Clark, R.Menikoff and D.H.Sharp, Phys.Rev. **D22** 3012 (1980).
- [32] R.P.Feynman and A.R.Hibbs, *Quantum Mechanics and Path Integrals* (McGraw Hill, New York, 1965).
- [33] V.P.Ermakov, Univ.Izv.Kiev **20** 1 (1880) ; E.Pinney, Proc.Am.Math.Soc.**1** 681 (1950).